About Shear Properties of Plain Weave Fabric CFRP at High Temperatures: Analytical and Experimental Approaches

Claudia Barile[1] [ID] **· Vimalathithan Paramsamy Kannan[1] · Alessandro Locasale[2] ·
Caterina Casavola[1]**

Abstract

The in-plane and interlaminar characteristics of plain weave fabric Carbon Fibre Rein-
forced Polymer (CFRP) composites are studied. The influence of the temperature expo-
sure, below the glass transition state of the composites, on these properties are studied. The
in-plane shear properties, shear strength and shear modulus are affected by the tempera-
ture exposure. The in-plane shear strength has dropped by 44.36% for the specimens tested
at 120 °C compared to the specimens tested at room temperature. The interlaminar shear
strength, however, are largely unaffected by the temperature exposure. The interlaminar
shear strength of the plain weave fabric CFRP largely depends on the cross-sectional area
of the specimen than the temperature exposure. Finally, several prediction models are used
for estimating the shear properties of the composites exposed to different temperatures.
Among them, Hawileh model fits very well with the experimental data for predicting the
in-plane shear strength, while Wang model fits well for the shear modulus. In addition to
these, fracture surfaces of the in-plane shear and interlaminar shear specimens are charac-
terized under optical microscopy to understand the failure modes and how they are influ-
enced by the temperature exposures.

1 Introduction

Carbon Fibre Reinforced Polymer (CFRP) composites have been abundantly used in vari-
ety of applications including aerospace, automotive and commercial industries. This is
due to their high strength-to-weight ratio, stiffness-to-weight ratio, resistance to various
chemicals and electrical insulation properties [1–7]. However, these specific strengths of

✉ Claudia Barile
  claudia.barile@poliba.it

1   Dipartimento di Meccanica, Matematica e Management, Politecnico di Bari, Via E. Orabona 4,
    70125 Bari, Italy

2   Blackshape S.p.A., 70043 Monopoli, Italy

the CFRP composites have significant advantages over the conventional isotropic materials only when they are loaded along the fibre direction [8–10]. The strength and stiffness of the CFRP decrease when the loading is off axis to the fibre direction [11, 12]. When a composite is loaded along the fibre axis, the fibres play a significant role in deciding the strength of the composite. However, when the composite is loaded off-axis to the fibre direction, several other factors such as matrix strength, fibre-matrix interface strength and interfacial strength between the plies play a crucial role in deciding their strength [13].

To improve the off-axis strength of the CFRP, several researchers have tried to implement variety of techniques. Most of these techniques involve modifications either in the matrix or the reinforcements [8, 9, 14–16]. FRP with plain weave fabric configuration have shown to have significant improvement in off-axis properties such as in-plane shear and interlaminar shear properties [8–10, 17].

Composites used in structural applications are often exposed to elevated temperatures, which decreases their mechanical properties. This is due to the significant differences in the thermal characteristics such as thermal conductivity, coefficient of thermal expansion and specific thermal capacity between the polymeric resin and the reinforcing fibres [18–20]. Several researchers have reported the significant reduction in mechanical properties of CFRP due to their exposure to elevated temperatures [2, 17, 21–27]. Various CFRP prepared from different thermosetting resins have shown to have lost their mechanical properties from 50 to 89% [22]. This reduction in mechanical properties is mostly based on the glass transition temperature (T_g) of the resin used, exposed temperature range and width-to-thickness ratio of the composites [24, 28, 29].

Since the off-axis properties such as shear properties are affected by the fibre-matrix interface, they are seriously affected when the composites are exposed to elevated temperature. Glass Fibre Reinforced Polymer (GFRP) composites with fibres in plain weave configuration shown to have lost 50% to 96% of their shear and flexural properties at elevated temperatures of 200 °C to 300 °C, respectively [23]. Their loss in properties can generally attributed to the type of resins used and their T_g.

Several research works have reported that the properties of CFRP tend to decrease when the exposure temperatures reach close to the T_g of the composites [21, 25, 30–32]. Some of the constitutional mechanical properties such as elastic modulus does not decrease significantly when the composites are tested below its T_g [22, 33, 34]. However, the in-plane shear properties tend to decrease even below the T_g of the composites. Therefore, the aim of this study is to understand the shear characteristics of the CFRP when they are exposed to temperatures below their T_g.

Apart from this, the in-plane shear properties, the shear strength, and shear modulus of the CFRP exposed to different temperatures are predicted using recently developed prediction models. A new hybrid model based on the research works by Gibson et al. [35] and Yu and Kodur [36] is proposed, and it is tested against the available prediction models in literature. The predicted results are compared with the experimental results for validation. Microscopic analysis on the fractured surface of the test specimens is performed to understand the failure modes and fracture behaviour of the CFRP. This research work aims at providing a comprehensive analysis on the shear properties of CFRP with plain weave fabrics exposed to elevated temperatures below the glass transition state of the composite.

2 Materials and Methods

2.1 Materials

Epoxy resin of density 1.267 g/cm^3 is used as the matrix for preparing the prepreg. Carbon fibre having a high tensile strength of 4900 MPa and a tensile modulus of 240 GPa is used as the reinforcement. The average density of the carbon fibre used is 1.8 g/cm^3. The reinforcements are configured in plain weave fabric configuration with the average fibre densities in warp and fill directions, respectively, are 1.78 g/cm^3 and 1.8 g/cm^3. The prepregs are prepared with a high fibre volume fraction of 58.5% and the area weight of 192 g/m^2.

Eight plies for in-plane shear test specimens, and twelve plies and sixteen plies for interlaminar shear test specimens, respectively are stacked with the same fibre direction in all the plies. Each of the ply has a nominal thickness of 0.218 mm. The stacked plies are packed in a vacuum bag with a pressure of 22 inches of Hg (minimum) and the entire setup is transferred to an oven, where the composite is cured. Initial curing is carried out at 132 °C, which is ramped at a rate of 3 °C/min and the composite is cured for about 120 to 150 min. Then the temperature is cooled down to 76 °C at a rate of 4.5 °C/min for post curing the composite. Finally, the composite panels are relieved from the vacuum.

The glass transition temperature T_g of the composites are taken from the supplier datasheet, where T_g is measured under the recommendations of ASTM D7028 – Standard Test Method for Glass Transition Temperature (DMA Tg) of Polymer Matrix Composites by Dynamic Mechanical Analysis (DMA). In the supplier datasheet, T_g is calculated from the storage modulus measured from DMA of the test specimens. The glass transition stage begins approximately around 134 °C and has an average T_g of 141 °C.

According to the ASTM D3518/D3518M – Standard Test Method for In-Plane Shear Response of Polymer Matrix Composite Materials by Tensile Test of a $\pm45°$ Laminate recommendations, end tabs must be used for the in-plane shear specimens. The end tabs are bonded to the specimens using Hysol EA9628 adhesive. The in-plane shear test specimens are cut from the composite panels in such a way that the fibres in the warp direction are 45° to the longitudinal (loading) direction.

17 short beam shear specimens from the panel of 12 plies and 16 specimens from the panel of 16 plies are cut according to ASTM D2334/D2334M – Standard Test Method for Short-Beam Strength of Polymer Matrix Composite Materials and Their Laminates. The short beam shear specimens are cut from the composite panels with the fibres in the warp direction run along the length of the specimens. The reason for using two different types of short beam shear specimen is to characterize the influence of the cross-sectional area and the elevated temperatures in the apparent interlaminar strength of the composite.

2.2 Test Methods

For characterizing the influence of the elevated temperatures on the in-plane shear properties of the plain weave fabric CFRP, 6 specimens are tested, respectively, at 4 different temperature conditions. The specimens are loaded in an INSTRON Servo-hydraulic testing machine with a 200 kN load cell. The entire setup is mounted inside an environmental chamber where the different temperature conditions are reached. A couple of uniaxial strain gauges are bonded to the test specimens tested at 100 °C and 120 °C along the longitudinal and transversal direction of the specimens. The test setup with the specimens
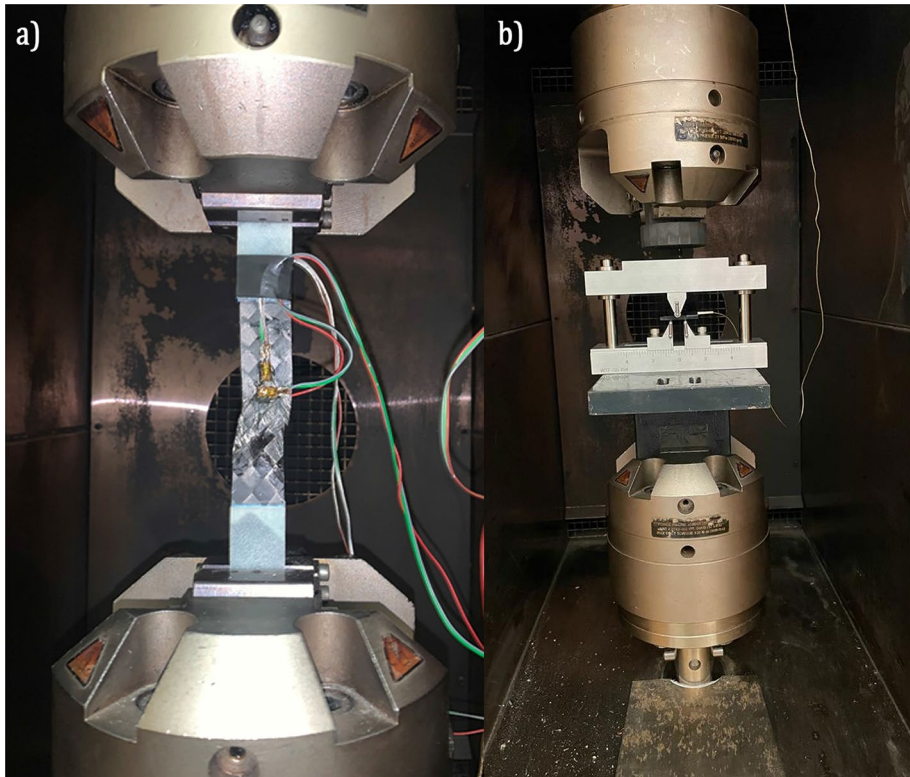
Fig. 1 Test Setup showing **a** Fractured In-Plane Shear Specimen mounted inside the environmental chamber with strain gauges **b** Short Beam Shear Test Setup inside the environmental chamber

mounted inside the environmental chamber is presented in Fig. 1a. The tests are carried out in displacement-controlled mode at a constant crosshead displacement velocity of 2.0 mm/min. The applied load, crosshead displacement, duration of the test, longitudinal strain and transversal strain are measured during the test.

The span length of the specimens, the loading nose and the supports of the short beam shear test are chosen as per the ASTM D2344/D2344M standard. The test setup for the short beam shear test is presented in Fig. 1b. 17 specimens cut from the panel of 12 plies are tested at room temperature. 6 specimens each from the panel of 16 plies are tested, respectively, at 100 °C and 120 °C. The experimental campaign is planned to understand the behaviour of the apparent interlaminar strength due to both the increase in thickness (and cross-sectional area) of the specimens and the operating temperature. Then the specimen is allowed to stay ideally at the designated temperature for 5 min inside the environmental chamber before the commencement of loading. The three-point bending load is applied on the test specimens at a constant crosshead displacement velocity of 1.0 mm/min.

More details about the number of specimens tested for the in-plane shear and the short beam shear tests are presented in Table 1.

The in-plane shear properties, the in-plane shear strength and shear modulus are calculated from the experimental data following the procedures indicated in ASTM standards.

Table 1 Test details and Specimen Details

Test Temperature	Type of Test	Width of the Specimen mm	Thickness of the Specimen mm	Denomination	Number of Test Specimens
Room Temperature	In-Plane Shear Test	24.76 ± 0.10	1.75 ± 0.6	IPS_30_00_n[a]	6
82 °C		24.72 ± 0.14	1.74 ± 0.02	IPS_82_00_n	6
100 °C		24.76 ± 0.10	1.75 ± 0.02	IPS_100_00_n	6
120 °C		24.78 ± 0.07	1.73 ± 0.07	IPS_120_00_n	6
Room Temperature	Short Beam Shear Test	5.2 ± 0.12	2.6 ± 0.06	SBS_30_00_n	17
100 °C		12.59 ± 0.04	3.53 ± 0.05	SBS_100_00_n	8
120 °C		12.60 ± 0.04	3.54 ± 0.03	SBS_120_00_n	6

[a] n indicates the number of the specimen tested

ASTM D3518/D3518 M – Standard Test Method for In-Plane Shear Response of Polymer Matrix Composite Materials by Tensile Test of a ± 45° Laminate recommendations are used for calculating the in-plane shear properties. The shear stress at the maximum applied load is taken as the in-plane shear strength of the test specimens. The in-plane shear strength τ_{12max} is calculated using Eq. (1), where P_{max} is the maximum load measured during the in-plane shear test of the specimen and A is its cross-sectional area.

$$\tau_{12max} = \frac{P_{max}}{2A} \tag{1}$$

The longitudinal ϵ_x and transversal strain ϵ_y values are measured during the in-plane shear test using the unidirectional strain gauges. The shear strain γ_{12i} at i^{th} point of the test data is calculated using Eq. (2).

$$\gamma_{12i} = \epsilon_{xi} - \epsilon_{yi} \tag{2}$$

The shear modulus G_{12} is calculated based on the chord modulus of elasticity method over the shear strain range of 2000 με and 5000 με, using Eq. (3).

$$G_{12} = \frac{\Delta\tau_{12}}{\Delta\gamma_{12}} \tag{3}$$

Similarly, the apparent interlaminar shear strength for the test specimens is calculated based on the recommendations from ASTM D2334/D2334M – Standard Test Method for Short-Beam Strength of Polymer Matrix Composite Materials and Their Laminates. The apparent interlaminar strength of the composites F^{sbs} are calculated using Eq. (4).

$$F^{sbs} = 0.75\frac{P_{max,sbs}}{bh} \tag{4}$$

where, $P_{max,sbs}$ is the maximum load observed during the short beam shear test and b and h are respectively the breadth and thickness of the test specimen. After testing, the fractured specimens are observed under optical microscope, Nikon SMZ-800 stereoscope at a resolution of 2560 pixels × 1920 pixels. The optical images of the fractured area of the in-plane shear and short beam shear specimens are observed to identify the damage modes which caused the catastrophic failure of the test specimens.

3 Predictive Model for Shear Properties at Elevated Temperature

All these prediction models for estimating the mechanical properties of composites at elevated temperatures can be traced back to the equation proposed by Henderson to describe the heat flow through an organic matrix [37]. The prediction models proposed for the mechanical properties generally assume that there is a strong link between the mechanical properties and two crucial variables: T_g and the residual resin content after decomposition. This is because the thermosetting resins used in structural materials have a single stage decomposition. First there will be a glass transition until the temperature reaches T_g, which will be followed by the commencement of decomposition [21]. While all the predictive models assume that the mechanical properties can be fitted to relationships similar to that of the modulus, the first model proposed was by Mahieux and Reifsnider [38, 39]. They have considered that when a polymer composite is a relaxed state (refers to the temperature state higher than T_g) or an

unrelaxed state (temperature state below T_g), the number of intermolecular bonds in the composite increases or decreases respectively. Based on that, they proposed a model, which is given in Eq. (5).

$$P(T) = P_R + (P_U - P_R)\exp\left[-\left(\frac{T}{T_0}\right)^m\right]$$

(5)

In their model, any elastic property of a composite $P(T)$ at the exposed temperature T can be predicted, if the property of the composite at relaxed state P_R and the property at unrelaxed state P_U are known. This model is based on the cumulative Weibull distribution as a function of temperature and the term m represents the Weibull exponent of the elastic property to be defined. The term T_0 represents the relaxation temperature of the composite. Mahieux and Reifsnider were able to predict different elastic properties of variety of polymers by setting the Weibull exponent values between 15 and 21 [38, 39].

The next model was proposed by Gibson et al. [35], which has become the basis of most of the prediction models used in the literature. Gibson et al. agreed with the theory of relaxed and unrelaxed state proposed by Mahieux and Reifsnider [38] but have found some instabilities in the model while processing some properties of the composite material. They improved the model by incorporating the glass transition state of the composite. Gibson et al. proposed to use the loss function (tanδ) obtained from the thermo-mechanical response of the material [35]. Based on the symmetrical shape of tanδ at the material relaxation stage, they improved the model in Eq. (5). Gibson model is presented in Eq. (6).

$$P(T) = R^n\left(\frac{P_U + P_R}{2} - \frac{P_U - P_R}{2}\tanh\left[k\left(T - T_g\right)\right]\right)$$

(6)

The constants R^n and k in Eq. (2), respectively, represents the residual resin content and the constant describing the breadth of the loss function distribution in thermo-mechanical response of the composite. When a material is in an undecomposed state, $R = 1$, while $R = 0$, when the material is completely decomposed. The power law relation R^n represents the extent of the resin percentage affecting the elastic property of the material.

Several researchers have tried to extrapolate these constants for their type of resin used or the type of elastic properties to be determined [22, 40, 41]. This led to the development of several other prediction models. The goal of this research work is to identify the model which can predict the shear properties of CFRP composites with fibres in plain weave fabric configuration.

For instance, Hawileh et al. [30] calibrated these constants using least square regression for predicting the tensile strength and elastic modulus of CFRP and Basalt Fibre Reinforced Polymer (BFRP) composites. The elastic properties of the composite at the exposed temperature T can be evaluated using Hawileh model using Eq. (7).

$$P(T) = P_U(0.594 - 0.405\tanh[0.017(T - 117.74)])$$

(7)

Nadjai et al. [42] proposed their model based on T_g of CFRP composites, which is presented in Eq. (8).

$$\frac{P(T)}{P_U} = \begin{cases} 1, & 0 \leq T < 100 \\ 1.267 - 0.00267T, & 100 \leq T < 475 \\ 0, & 475 \leq T \end{cases}$$

(8)

Wang et al. [18] improvised the model proposed by Chen and Young [43, 44] for estimating the stress-exposed temperature relationship in metals and adopted it to CFRP. Their model is robust for many elastic properties, which is presented in Eq. (9).

$$\frac{P(T)}{P_U} = \begin{cases} 1 - \frac{(T-22)^{0.9}}{200}, & 12 \leq T < 150 \\ 0.59 - \frac{(T-150)^{0.7}}{490}, & 100 \leq T < 420 \\ 0.48 - \frac{(T-420)^{1.8}}{76000}, & 420 \leq T < 706 \end{cases} \tag{9}$$

One of the versatile models were proposed by Yu and Kodur [36], which is based on the Gibson model in Eq. (2). To obtain the property retention percentage of any elastic properties, Eq. (6) must be divided by the said property at the unrelaxed stage P_U. Their model is presented in Eq. (10).

$$\frac{P(T)}{P_U} = \frac{1 + {}^{P_R}/_{P_U}}{2} - \frac{1 - {}^{P_R}/_{P_U}}{2} \tanh\left[k(T - T_g)\right] \tag{10}$$

This model, however, is based on the assumption that the defined property $P(T)$ is largely based on the fibre orientations and therefore the constant R is assumed to be 1. The constant k can be calculated through linear least square regression analysis of large experimental data. This model is named as modified Gibson model in this research work.

The in-plane shear strength and the shear modulus are the only properties predicted in this study using the aforementioned models. These predicted values are compared with the experimental results.

4 Results and Discussions

4.1 In-Plane Shear Properties of Plain Weave Fabric CFRP at Elevated Temperatures

The in-plane shear test specimens are tested at four different temperature conditions. The in-plane shear properties, the shear strength and modulus of the test specimens are presented in Fig. 2 and Table 2. According to the ASTM D3518/D3518M standard, the shear
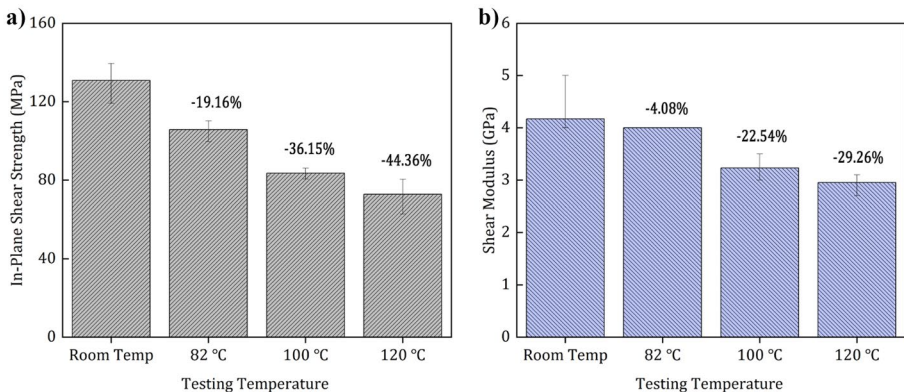

Fig. 2 Variation in In-Plane Shear properties **a** In-Plane Shear Strength and **b** Shear Modulus of CFRP tested at different temperatures

Table 2 In-Plane Shear Strength and Shear Modulus of Specimens tested at four different temperatures: Room temperature, 82 °C, 100 °C and 120 °C

Specimen Name	In-Plane Shear Strength	Shear Modulus
	MPa	*GPa*
Tested at room temperature		
IPS_30_001	132.93	4.00
IPS_30_002	131.26	5.00
IPS_30_003	119.13	4.00
IPS_30_004	135.00	4.00
IPS_30_005	139.52	4.00
IPS_30_006	127.04	4.00
Mean	*130.81*	*4.17*
Std.dev	*7.05*	*0.41*
Tested at 82 °C		
IPS_82_001	107.62	4.00
IPS_82_002	106.36	4.00
IPS_82_003	101.56	4.00
IPS_82_004	109.17	4.00
IPS_82_005	110.24	4.00
IPS_82_006	99.53	4.00
Mean	*105.75*	*4.00*
Std.dev	*4.29*	*-*
Tested at 100 °C		
IPS_100_001	85.54	3.00
IPS_100_002	84.08	3.00
IPS_100_003	80.51	3.50
IPS_100_004	82.29	3.10
IPS_100_005	82.67	3.20
IPS_100_006	86.01	3.30
Mean	*83.52*	*3.23*
Std.dev	*2.09*	*0.18*
Tested at 120 °C		
IPS_120_001	72.84	2.70
IPS_120_002	62.76	3.00
IPS_120_003	76.85	2.90
IPS_120_004	68.64	2.90
IPS_120_005	75.19	3.10
IPS_120_006	80.42	3.10
Mean	*72.78*	*2.95*
Std.dev	*6.30*	*0.15*

strength is considered as the shear stress at failure of the test specimens. In the composites with fibres in plain weave fabric configurations, the specimen may carry load even after failure as the overlapping fibres in the warp and weft direction prevent the explosive failure. Some unbroken fibre strands align themselves to the loading direction and carried the load before final failure of the specimens. Therefore, the maximum shear stress in the test specimen for the applied load is taken as its shear strength. The shear modulus is taken as the chord modulus of the test over the shear strain range of 2000 με and 5000 με.

Several researchers have tested different types of Fibre Reinforced Polymer (FRP) composites, including CFRP, BFRP and Glass-FRP (GFRP) composites and have shown that the loading along the axis of the fibres do not decrease the mechanical properties significantly when the exposed temperature is below T_g [32, 33, 45]. The consensus is that the fibres have high resistance to heat, and consequently, the tensile properties, which are predominantly governed by the fibre strength, are not affected by the exposed temperature. However, when the loading is off-axis to the fibres, (in this case of in-plane shear specimens), different failure modes such as delamination and fibre-matrix debonding occur in the test specimen [13, 14]. The properties of the polymeric resin matrix play a crucial role in these failure modes and consequently, the materials start to lose their properties at elevated temperatures.

This can be observed in the test results presented in Fig. 2. The in-plane shear strength and modulus of the specimens tested at room temperature are 130.81 MPa and 4.17 GPa, respectively. These properties decrease gradually when the exposed temperature is increased. The test specimens exposed to 120 °C show an in-plane shear strength of 72.78 MPa and a shear modulus of 2.95 GPa. The reduction in in-plane shear strength is accounted for 19.16%, 36.15% and 44.36%, respectively, for the test specimens exposed to 82 °C, 100 °C and 120 °C. Similarly, the shear modulus has decreased by 4.08%, 22.54% and 29.26% for the specimens exposed to 82 °C, 100 °C and 120 °C, respectively. The test specimens lose almost half their in-plane shear strength when tested at 120 °C, which is close to the T_g of the plain weave fabric CFRP (142 °C).

The fractured in-plane shear specimens are shown in Fig. 3. It has been shown by Wisnom et al. [13] that the in-plane shear failure modes initiate from the vertical free edges of the test specimen, and it propagates along the axis of the fibre direction. This can be observed in Fig. 3. Due to the plain weave fabric FRP, the woven fibres hold the longitudinal fibres together, preventing the explosive failure of the composites [21].
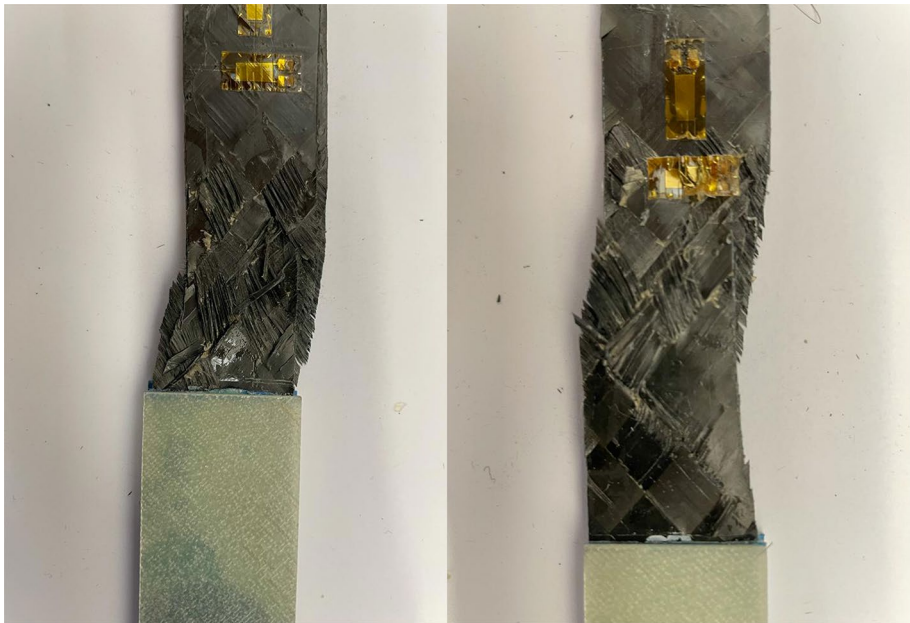

Fig. 3 CFRP specimens failed under Shear Load, but the Fibres are held together due to the Plain Weave configuration

The fractured specimens are further analysed under optical microscope and the microscopic images of the fractured areas are presented in Fig. 4. Since the failure of the test specimens did not result in an explosive failure, segmenting the small section of the material for fractographic analysis under Scanning Electron Microscope (SEM) will lead to loss of data. Therefore, the fractographic analysis is performed under optical microscope. The fracture surface shows three distinct characteristics. First, the fibres are fractured yet holding the specimen from explosive failure; second, the crack propagating along the width of the specimen on the axis of the fibre direction and finally, the evidence of delamination in resin rich area. The delamination in the resin rich area could possibly explain the decrease in in-plane shear strength and modulus of the test specimens exposed to higher temperatures. According to Wisnom et al. [13] and Tessema et al. [14], during the initial stages of off-axis loading, the matrix material takes a part of the load, while the fibre rotates and tries to align itself to the loading direction. This causes the dips and bumps present in the plain weave fabric to shrink, squeeze the matrix material [14]. The larger difference between the coefficient of thermal expansion of the resin matrix and the fibres are well-known. This could have influenced the material to start failing at the resin rich areas at higher temperatures and promoted the delamination failure. Apart from this, the initial stage of loading largely affects the matrix material. These could have been the reason why the specimens tested at 120 °C lost about 44.36% of their in-plane shear strength with respect to the specimens tested at room temperature.

To further establish the influence of matrix in the failure of the specimens, the shear stress-shear strain curves of the test specimens exposed to 100 °C and 120 °C are compared. The shear stress values corresponding only up to a strain of 4000 $\mu\varepsilon$ is taken for analysis and are
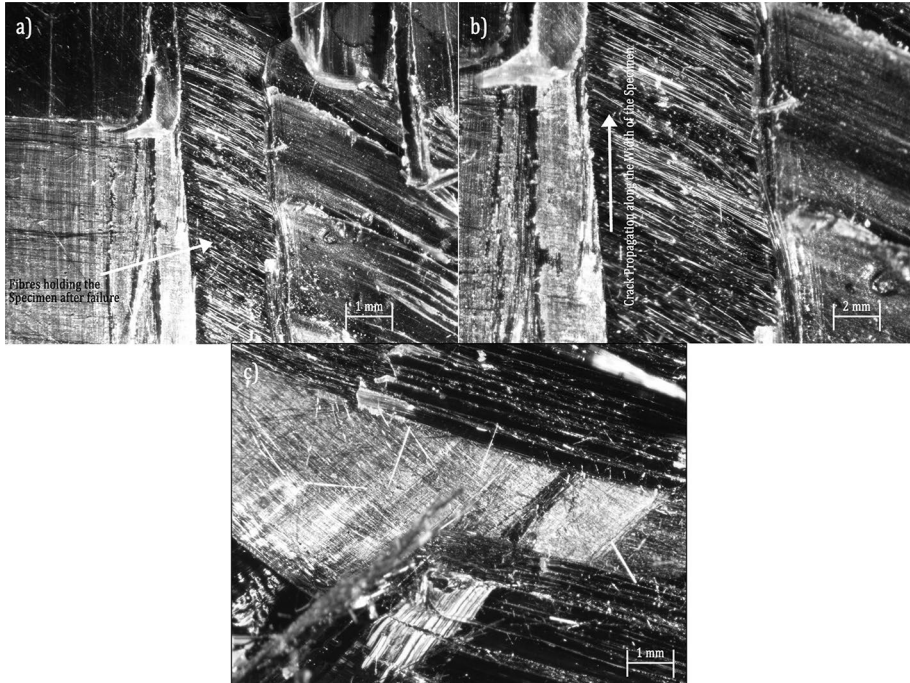

Fig. 4 Fracture areas of the In-Plane Shear Test Specimens showing **a** Fibres holding the Specimen after Failure **b** Crack Propagation Direction along the Width and **c** Delaminated Area

shown in Fig. 5. The average shear stress of the specimens tested at 100 °C at 4000 με is 14.62 MPa while the average shear stress of the specimens tested at 120 °C at 4000 με is 13.76 Mpa. During the initial stages of loading, the specimens tested at 120 °C show a shear stress 5.87% less than the specimens tested at 100 °C. This reduction is slightly lower than the average reduction of shear stress and shear modulus between these two specimens at failure, which is 8.21% and 6.71%, respectively. As discussed earlier, during the initial stages of off-axis loading, most of the load is carried by the matrix, while the fibres try to align itself to the loading direction. Therefore, it can be considered that matrix material carried a significant amount of load during these initial stages. Since the shear stress values of the specimens tested at 100 °C at 4000 με is 5.87% more than the shear stress of the specimens tested at 120 °C, it could be considered as the influence of matrix material. Since the overall reduction in in-plane shear strength and shear modulus of the test specimens tested at 100 °C and 120 °C is slightly greater than the reduction of the shear stress at early stages, it can be considered that the matrix material plays a crucial role in determining the overall in-plane shear properties of the material.

4.2 Prediction Model for In-Plane Shear Properties at Elevated Temperatures

The in-plane shear properties, shear modulus and in-plane shear strength are predicted for different elevated temperatures using four different prediction models: Hawileh model, Wang model, Nadjai model, and Modified Gibson model.

For the Modified Gibson model proposed in Eq. (6), the in-plane shear strength of the composite at relaxed state is required. The relaxed state refers to the temperature above the glass transition state. In this study, however, the specimens are tested only below the glass transition state. Therefore, the in-plane shear strength at relaxed state is unavailable. However, based on the consideration that these models are based on two important resin characteristics, T_g and the residual resin content percentage, the in-plane shear strength of CFRP with similar T_g is taken from literature [21] and used in Eq. (10). Then by using linear regression solver, the value of the constant k is calculated to be 0.039. This is used for predicting the in-plane shear properties using modified Gibson model.

The in-plane shear strength predicted using different models are presented in Fig. 6. It can be observed that the experimental data fits well with the Hawileh model. The

Fig. 5 Shear Stress-Shear Strain Curves of Specimens tested at 100 °C and 120 °C
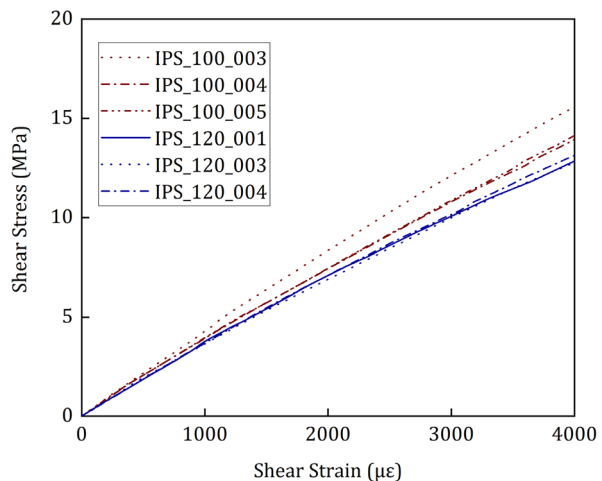
maximum difference between the experimental data and the Hawileh model is at 100 °C, where the predicted data is around 13.1% higher. The predicted value of Hawileh model is just 2.75% greater than the experimental data at 82 °C. Although the Wang model predicts the shear strength at 82 °C at a difference of just 0.70%, its prediction value deviates at higher temperatures. The predicted values at 100 °C and 120 °C are 18.68% and 25.72%, respectively, higher than the experimental data. Nadjai model, Gibson model and modified Gibson model has higher difference between the prediction and experimental value, which is generally greater than 50%. Considering these observations, Hawileh model fits well with the experimental data.

However, the shear modulus of the plain weave fabric CFRP do not coincide with the predicted values by Hawileh model or any other models except the model by Wang et al. [18]. The predicted shear modulus by Wang model is merely 3.47% and 2.43% greater than the experimental values at 100 °C and 120 °C, respectively. Indeed, the predicted shear modulus at 82 °C is 15.89% greater the experimental data, however, the minimum percentages in other models (Nadjai, Gibson and modified Gibson) exceed 12% to 33% at temperatures 100 °C and 120 °C. It can be observed in Fig. 7 that the predicted values by Hawileh et al. are slightly less than the experimental shear modulus at 100 °C, which is 8% greater however, the difference is larger at 120 °C (18.23%). Wang et al. proposed their models based on the stress-temperature relationship in metals and refined the constants for CFRP composites [18, 43]. Since the retention of modulus in CFRP composites (both tensile and shear modulus) is quite higher than the retention of tensile strength/shear strength, their model probably suits the prediction of shear modulus. From these observations, it can be said that for predicting the in-plane shear strength, Hawileh model can be used but for predicting shear modulus Wang model can be used.

4.3 Interlaminar Shear Strength of Plain Weave Fabric CFRP Composites at Elevated Temperatures

The apparent interlaminar strength of the composites are presented and discussed in this section. As mentioned in Section 2.2, the influence of the cross-sectional area and the temperature exposure on the apparent interlaminar strength is discussed in this section.

Fig. 6 In-Plane Shear Strength of the CFRP specimens predicted for different testing temperatures using different prediction models
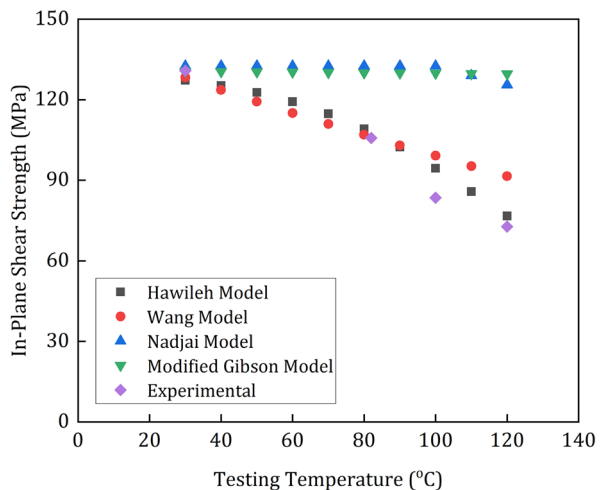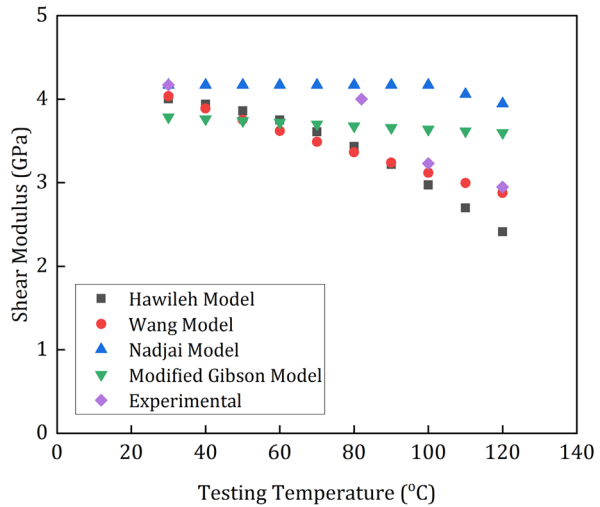
Fig. 7 Shear Modulus of the CFRP specimens predicted for different testing temperatures using different prediction models

The term 'apparent' is used often before the interlaminar strength; this is because there is always a concern about the shear stress distribution and the occurrence of other failure modes in the short beam shear test [13]. Nonetheless, the interlaminar shear strength obtained using short beam shear strength is comparatively significant.

A total of 17 specimens are tested at room temperature, and 8 specimens at 100 °C and 6 specimens at 120 °C. It must be noted that the cross-sectional areas of the three groups of specimens are different, which are highlighted in Table 1. The average interlaminar shear strength obtained from the short beam shear tests are presented in Fig. 8.

The interlaminar shear strength of the specimens tested at 100 °C and 120 °C are apparently similar. The increase in temperature does not have any significant effect on the interlaminar strength of the composite. The CFRP composites tested at room temperature has a lower cross-sectional area, and it has an average interlaminar shear strength of 58.1 MPa, which is less than both the specimens tested at 100 °C and 120 °C.

To find the extent of the influence of temperature and cross-sectional area on the interlaminar shear strength, two-way ANOVA analysis is carried out on the data obtained from the 31 specimens [46, 47]. The analysis is aimed at understanding the effects of the two independent parameters, the cross-sectional area, and the exposure temperature, on the interlaminar shear strength of the composites. The ANOVA results are presented in Fig. 9.

It can be seen from the ANOVA results in Fig. 9 that the cross-sectional area of the composites contributes about 86% of the variation in the interlaminar shear strength. This has been corroborated in several research works that the outer ply serves a protective layer and resists the interlaminar failure occurring in the midplane [24, 28, 29, 48, 49]. Therefore, the specimen with lower cross-sectional area shows less interlaminar strength than the other two specimens. The reason for less variation in interlaminar strength due to the temperature exposure can be explained as follows. The interlaminar failure occurs generally in the midplane of the other interlayers away from the outer plies. During the temperature exposure at 100 °C and 120 °C, the outer plies serve as an insulator and prevent the heat to be transferred to the midplane. This probably has prevented the failure mechanism to be affected by the exposure temperature. Consequently, the interlaminar shear strength of the composites are not affected due to the exposure

Fig. 8 Interlaminar Shear Strength of Specimens tested at Room Temperature, 100 °C and 120 °C
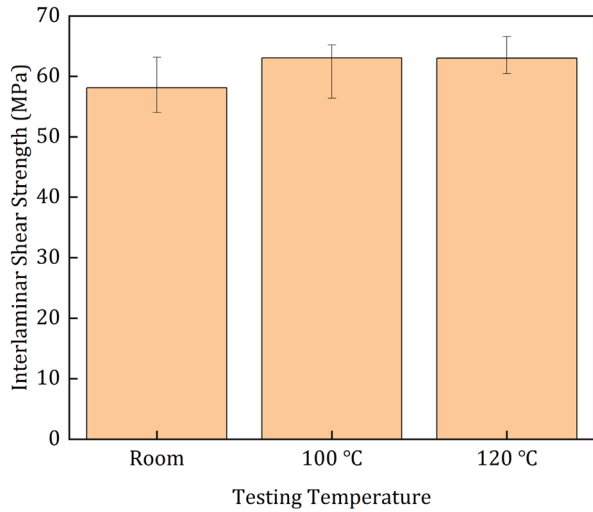
temperature. This could be the reason why there is a little difference in interlaminar shear strength of the CFRP tested at 100 °C and 120 °C.

To validate the observations made on the interlaminar shear strength, the microscopic images of the untested specimen are presented in Fig. 10 and the fractured surfaces of the tested specimens are presented in Fig. 11.

In all the tested specimens, several failure modes have contributed to the catastrophic failure of the specimens. All these failure modes are normally observed in short beam shear test according to ASTM D2344/D2344M standards, and also observed in literature [47]. In all the specimens, the flexural failure by tension occurred in the surface opposite to the loading face of the specimen along the loading axis (Fig. 11a). Apart

Fig. 9 ANOVA results for the Interlaminar Strength of the Plain Weave Fabric based on the Contributions of Temperature and Cross-Sectional Area
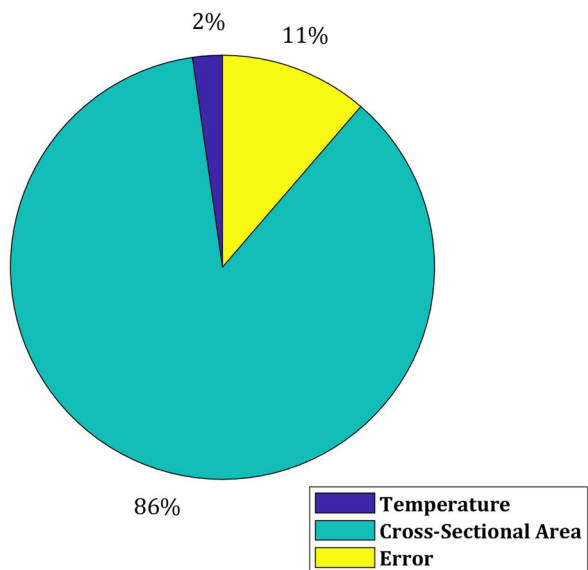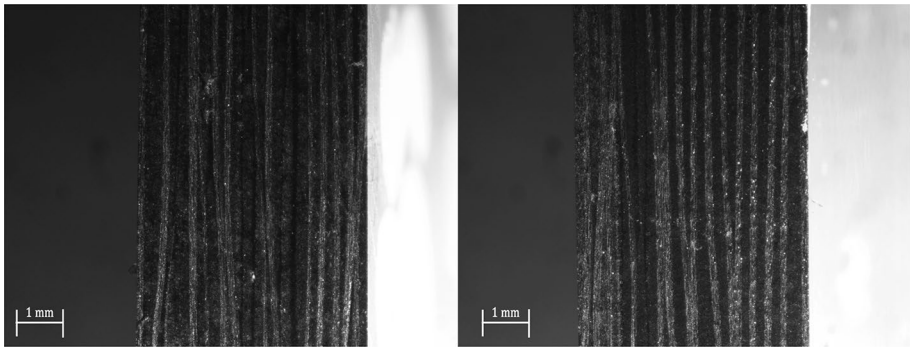
Fig. 10 Optical Microscopy Images of Untested Specimen showing resin rich area

from these, there are some through-thickness cracks, which originate from the resin rich region and propagates through the thickness of the composite (Fig. 11b). The untested specimen shows that there are several resin rich regions in the specimen through the thickness of the specimen (Fig. 10). These regions serve as the initiators for through-thickness crack growth. Despite the through-thickness cracks, explosive failure did not occur in the specimens, as the warp fibres hold the longitudinal fibres together.

Apart from these, there are some interlayer cracks near the mid plane of the specimens, which also occurs in the resin rich region (Fig. 11c). The major failure, however,
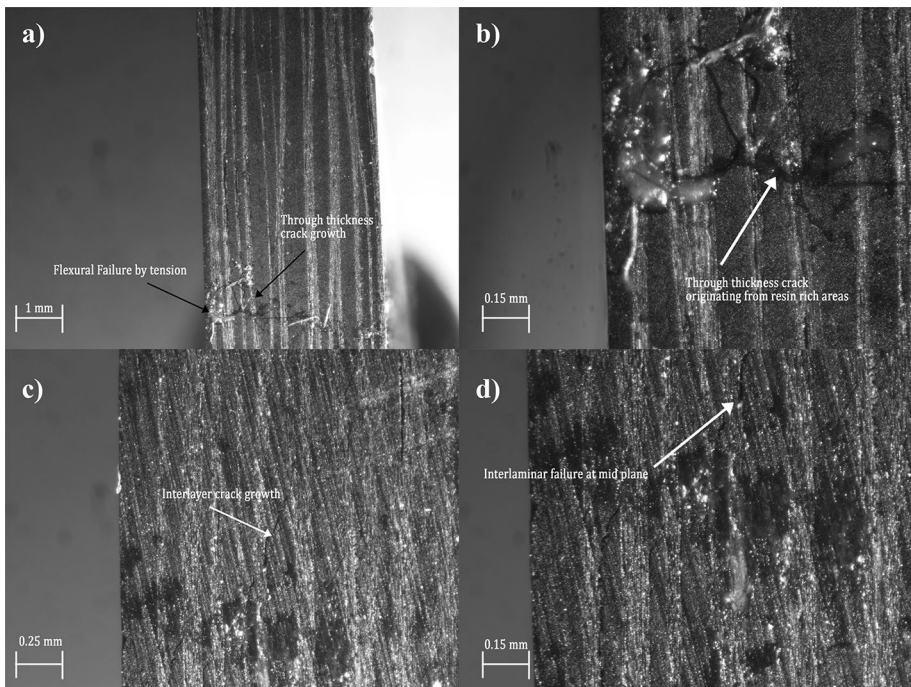

Fig. 11 Optical Microscopic Images showing the Fractured Areas **a** Flexural Failure by Tension **b** Exploded View showing the through-thickness crack growth originating from the resin rich regions **c** Inter Layer crack growth in resin rich regions **d** Interlaminar Failure at mid plane

is the interlaminar failure, which occurs in the mid plane of the specimen and propagates along the length of the specimen. Several microcracks and inter layer cracks that can be observed also occurred away from the outer plies. This indicates that the major failure occurred near the mid plane of the specimen, and the temperature exposure could not have had a greater influence.

Summarizing the observations made so far, the in-plane shear strengths of the specimen are largely affected by the temperature exposure, while the interlaminar shear strength of the plain weave fabric CFRP remains unaffected due to the exposed temperature. It must be noted that this holds true when the exposed temperature is less that the T_g of the specimen.

5 Conclusion

Plain weave fabric CFRP specimens are tested at elevated temperatures to study the in-plane shear and interlaminar shear properties. The in-plane shear properties, the in-plane shear strength and interlaminar shear strength are greatly affected by the exposed temperature, even when the temperature is below the T_g of the composites. This is due to the matrix carrying most of the load during the initial stages of loading and consequently affecting the off-axis load bearing characteristics of the composites. The failure occurrences, which occurs mostly in the resin rich region, in delamination mode is also the reason for this reduction in in-plane shear properties at elevated temperatures. The prediction model, Hawileh model can be used for estimating the in-plane shear strength, while Wang model can be used for estimating the shear modulus of the plain weave fabric CFRP at different temperature exposures. The interlaminar strength of the composite is largely unaffected by the exposure to elevated temperatures. Nonetheless, the variation in cross-sectional area of the composites affect them greatly. Both of these can be attributed to the protection provided by the outer plies, which insulates the heat flow through the composites and retaining the interlaminar properties at elevated temperatures. The failure modes occurring in plies away from the outer plies show that the thickness clearly influences the interlaminar strength of the composites.

Author Contributions Claudia Barile – Conceptualization, Methodology, Validation, Formal Analysis, Data Curation and Writing – Review & Editing; Vimalathithan Paramsamy Kannan – Conceptualization, Methodology, Validation, Formal Analysis, Data Curation, Writing – Original Draft and Writing – Review & Editing; Alessandro Locasale – Data Curation and Supervision; Caterina Casavola – Supervision**.**

Data Availability The raw/processed data required to reproduce these findings cannot be shared at this time as the data also forms part of an ongoing study.

Declarations

Competing Interests The authors have no competing interests to declare that are relevant to the content of this article. The authors have no relevant financial or non-financial interests to disclose. All authors certify that they have no affiliations with or involvement in any organization or entity with any financial interest or non-financial interest in the subject matter or materials discussed in this manuscript. The authors have no financial or proprietary interests in any material discussed in this article.

References

1. Liu, T., Liu, X., Feng, P.: A comprehensive review on mechanical properties of pultruded FRP composites subjected to long-term environmental effects. Compos. B. Eng. **191**, 107958 (2020)
2. Feng, P., Wang, J., Wang, Y., Loughery, D., Niu, D.: Effects of corrosive environments on properties of pultruded GFRP plates. Compos. B. Eng. **67**, 427–433 (2014)
3. Alsayed, S., Al-Salloum, Y., Almusallam, T., El-Gamal, S., Aqel, M.: Performance of glass fiber reinforced polymer bars under elevated temperatures. Compos. B. Eng. **43**, 2265–2271 (2012)
4. Alves, J., El-Ragaby, A., El-Salakawy, E.: Durability of GFRP bars' bond to concrete under different loading and environmental conditions. J. Compos. Constr. **15**, 249–262 (2011)
5. Miyano, Y., Mcmurray, M.K., Kitade, N., Nakada, M., Mohri, M.: Role of matrix resin on the flexural static behavior of unidirectional pitch-based carbon fiber laminates. Adv. Compos. Mater. **4**, 87–99 (1994)
6. Miyano, Y., Nakada, M., Kudoh, H., Muki, R.: Prediction of tensile fatigue life under temperature environment for unidirectional CFRP. Adv. Compos. Mater. **8**, 235–246 (1999)
7. Kobayashi, S., Suna, K., Yasuda, T.: Mechanical properties and fracture behavior of nonwoven fabric reinforced plastics for rehabilitation of sewage pipes. Adv. Compos. Mater. **21**, 413–423 (2012)
8. Kim, J., Shioya, M., Kobayashi, H., Kaneko, J., Kido, M.: Mechanical properties of woven laminates and felt composites using carbon fibers. Part 2: interlaminar properties. Compos. Sci. Technol. **64**, 2231–2238 (2004)
9. Kim, J., Shioya, M., Kobayashi, H., Kaneko, J., Kido, M.: Mechanical properties of woven laminates and felt composites using carbon fibers. Part 1: in-plane properties. Compos. Sci. Technol. **64**, 2221–2229 (2004)
10. Kotaki, M., Hamada, H.: Effect of interfacial properties and weave structure on mode I interlaminar fracture behaviour of glass satin woven fabric composites. Compos. A. Appl. Sci. Manuf. **28**, 257–266 (1997)
11. Kumar, P., Singh, R.K.: Impact damage area and interlaminar toughness of modified FRP laminates. Adv. Compos. Mater. **9**, 77–88 (2000)
12. Amagi, S., Wajima, M., Miyano, Y.: Flexural fracture behavior of carbon/aramid hybrid unidirectional reinforced FRP. Adv. Compos. Mater. **2**, 307–318 (1992)
13. Wisnom, M.R., Jones, M.I.: A comparison between interlaminar and in-plane shear strength of unidirectional glass fibre-epoxy. Adv. Compos. Lett. **3**, 096369359400300205 (1994)
14. Tessema, A., Mitchell, W., Koohbor, B., Ravindran, S., van Tooren, M., Kidane, A.: The effect of nano-fillers on the in-plane and interlaminar shear properties of carbon fiber reinforced composite. J. Dyn. Behav. Mater. **4**, 296–307 (2018)
15. Yamamoto, T., Hyakutake, H.: Comparison of strength and damage for notched FRP plates made by injection molding with that from machining. Adv. Compos. Mater. **11**, 351–363 (2002)
16. Touhari, M., Mitiche-Kettab, R., Bali, A.: Behavior and new strength model of FRP square columns based on the FRP effective circumferential failure and the effective lateral confining pressure. Adv. Compos. Mater. **30**, 222–242 (2021)
17. Jafari, A., Bazli, M., Ashrafi, H., Oskouei, A.V., Azhari, S., Zhao, X.-L., Gholipour, H.: Effect of fibers configuration and thickness on tensile behavior of GFRP laminates subjected to elevated temperatures. Constr. Build. Mater. **202**, 189–207 (2019)
18. Wang, K., Young, B., Smith, S.T.: Mechanical properties of pultruded carbon fibre-reinforced polymer (CFRP) plates at elevated temperatures. Eng. Struct. **33**, 2154–2161 (2011)
19. Wong, P.M.H., Wang, Y.C.: An experimental study of pultruded glass fibre reinforced plastics channel columns at elevated temperatures. Compos. Struct. **81**, 84–95 (2007)
20. Wong, P.M.H., Davies, J.M., Wang, Y.C.: An experimental and numerical study of the behaviour of glass fibre reinforced plastics (GRP) short columns at elevated temperatures. Compos. Struct. **63**, 33–43 (2004)
21. Jarrah, M., Najafabadi, E.P., Khaneghahi, M.H., Oskouei, A.V.: The effect of elevated temperatures on the tensile performance of GFRP and CFRP sheets. Constr. Build. Mater. **190**, 38–52 (2018)
22. Bazli, M., Abolfazli, M.: Mechanical properties of fibre reinforced polymers under elevated temperatures: an overview. Polymers. **12**, 2600 (2020)

23. Ashrafi, H., Bazli, M., Jafari, A., Ozbakkaloglu, T.: Tensile properties of GFRP laminates after exposure to elevated temperatures: effect of fiber configuration, sample thickness, and time of exposure. Compos. Struct. **238**, 111971 (2020)
24. Ashrafi, H., Bazli, M., Najafabadi, E.P., Oskouei, A.V.: The effect of mechanical and thermal properties of FRP bars on their tensile performance under elevated temperatures. Constr. Build. Mater. **157**, 1001–1010 (2017)
25. Bazli, M., Ashrafi, H., Jafari, A., Zhao, X.-L., Raman, R.K., Bai, Y.: Effect of fibers configuration and thickness on tensile behavior of GFRP laminates exposed to harsh environment. Polymers. **11**, 1401 (2019)
26. Bazli, M., Ashrafi, H., Jafari, A., Zhao, X.-L., Gholipour, H., Oskouei, A.V.: Effect of thickness and reinforcement configuration on flexural and impact behaviour of GFRP laminates after exposure to elevated temperatures. Compos. B. Eng. **157**, 76–99 (2019)
27. Barile, C., Casavola, C., Pappalettere, C., Tursi, F.: RFI composite materials behaviour. Struct. Integr. Life. **10**, 209–213 (2010)
28. Hamad, R.J.A., Johari, M.A.M., Haddad, R.H.: Mechanical properties and bond characteristics of different fiber reinforced polymer rebars at elevated temperatures. Constr. Build. Mater. **142**, 521–535 (2017)
29. Naser, M., Hawileh, R., Rasheed, H.: Modeling fire response of RC beams strengthened with CFRP laminates. Spec. Publ. **301**, 1–18 (2015)
30. Hawileh, R.A., Abdalla, J.A., Hasan, S.S., Ziyada, M.B., Abu-Obeidah, A.: Models for predicting elastic modulus and tensile strength of carbon, basalt and hybrid carbon-basalt FRP laminates at elevated temperatures. Constr. Build. Mater. **114**, 364–373 (2016)
31. Cao, S., Wang, X., Wu, Z.: Evaluation and prediction of temperature-dependent tensile strength of unidirectional carbon fiber-reinforced polymer composites. J. Reinf. Plast. Compos. **30**, 799–807 (2011)
32. Cao, S., Zhis, W.U., Wang, X.: Tensile properties of CFRP and hybrid FRP composites at elevated temperatures. J. Compos. Mater. **43**, 315–330 (2009)
33. Reis, J.M.L., Coelho, J.L.V., Monteiro, A.H., da Costa Mattos, H.S.: Tensile behavior of glass/epoxy laminates at varying strain rates and temperatures. Compos. B. Eng. **43**, 2041–2046 (2012)
34. Hawileh, R.A., Abu-Obeidah, A., Abdalla, J.A., Al-Tamimi, A.: Temperature effect on the mechanical properties of carbon, glass and carbon–glass FRP laminates. Constr. Build. Mater. **75**, 342–348 (2015)
35. Gibson, A.G., Wu, Y.-S., Evans, J.T., Mouritz, A.P.: Laminate theory analysis of composites under load in fire. J. Compos. Mater. **40**, 639–658 (2006)
36. Yu, B., Kodur, V.: Effect of temperature on strength and stiffness properties of near-surface mounted FRP reinforcement. Compos. B. Eng. **58**, 510–517 (2014)
37. Henderson, J.B., Wiebelt, J.A., Tant, M.R.: A model for the thermal response of polymer composite materials with experimental verification. J. Compos. Mater. **19**, 579–595 (1985)
38. Mahieux, C.A., Reifsnider, K.L.: Property modeling across transition temperatures in polymers: application to thermoplastic systems. J. Mater. Sci. **37**, 911–920 (2002)
39. Mahieux, C.A., Reifsnider, K.L., Case, S.W.: Property modeling across transition temperatures in PMC's: Part I. Tensile properties. Appl. Compos. Mater. **8**, 217–234 (2001)
40. Saafi, M.: Effect of fire on FRP reinforced concrete members. Compos. Struct. **58**, 11–20 (2002)
41. Firmo, J.P., Correia, J.R., Bisby, L.A.: Fire behaviour of FRP-strengthened reinforced concrete structural elements: a state-of-the-art review. Compos. B. Eng. **80**, 198–216 (2015)
42. Nadjai, A., Talamona, D., Ali, F.: Fire performance of concrete beams reinforced with FRP bars, pp. 401–410. Proceeding of the Int. Sympsium on Bond Behaviour of FRP in Structures (2005)
43. Chen, J., Young, B.: Stress–strain curves for stainless steel at elevated temperatures. Eng. Struct. **28**, 229–239 (2006)
44. Chen, J., Young, B.: Experimental investigation of cold-formed steel material at elevated temperatures. Thin-Walled. Structures. **45**, 96–110 (2007)
45. Chowdhury, E.U., Eedson, R., Bisby, L.A., Green, M.F., Benichou, N.: Mechanical characterization of fibre reinforced polymers materials at high temperature. Fire. Technol. **47**, 1063–1080 (2011)
46. Wu, C.F.J., Hamada, M.: Experiments: planning, analysis, and parameter design optimization. Wiley, New York (2000)
47. Neter, J., Kutner, M.H., Nachtsheim, C.J., Wasserman, W.: Applied linear statistical models, 4th edn. Irwin Press, US (1996)
48. Hawileh, R.A., Rasheed, H.A.: Thermal analysis of GFRP-reinforced continuous concrete decks subjected to top fire. Int. J. Adv. Struct. Eng. **9**, 315–323 (2017)
49. Baran, I.J., Nowak, M.B., Chłopek, J.P., Konsztowicz, K.J.: Acoustic emission from microcrack initiation in polymer matrix composites in short beam shear test. J. Nondestr. Eval. **37**, 1–10 (2018)